

Single particle tracking in systems showing anomalous diffusion: the role of weak ergodicity breaking

Stas Burov,^{1,*} Jae-Hyung Jeon,² Ralf Metzler,^{2,†} and Eli Barkai^{1,‡}

¹*Department of Physics, Bar Ilan University, Ramat-Gan 52900, Israel*

²*Physics Department, Technical University of Munich, D-85747 Garching, Germany*

Anomalous diffusion has been widely observed by single particle tracking microscopy in complex systems such as biological cells. The resulting time series are usually evaluated in terms of time averages. Often anomalous diffusion is connected with non-ergodic behaviour. In such cases the time averages remain random variables and hence irreproducible. Here we present a detailed analysis of the time averaged mean squared displacement for systems governed by anomalous diffusion, considering both unconfined and restricted (corrallated) motion. We discuss the behaviour of the time averaged mean squared displacement for two prominent stochastic processes, namely, continuous time random walks and fractional Brownian motion. We also study the distribution of the time averaged mean squared displacement around its ensemble mean, and show that this distribution preserves typical process characteristic even for short time series. Recently, velocity correlation functions were suggested to distinguish between these processes. We here present analytical expressions for the velocity correlation functions. Knowledge of the results presented here are expected to be relevant for the correct interpretation of single particle trajectory data in complex systems.

PACS numbers: 02.50.-r, 05.40.Fb, 05.10.Gg

I. INTRODUCTION

Single particle tracking microscopy provides the position time series $\mathbf{r}(t)$ of individual particle trajectories in a medium [1–4]. The information garnered by single particle tracking yields insights into the mechanisms and forces, that drive or constrain the motion of the particle. An early example of systematic single particle tracking is given by the work of Jean Perrin on diffusive motion [5]. Due to the relatively short individual trajectories, Perrin used an ensemble average over many trajectories to obtain meaningful statistics. A few years later, Nordlund conceived a method to record much longer time series [6], allowing him to evaluate individual trajectories in terms of the time average and thus to avoid averages over not perfectly identical particles. Today, single particle tracking has become a standard tool to characterise the microscopic rheological properties of a medium [7], or to probe the active motion of biomolecular motors [8]. Particularly in biological cells and complex fluids single particle trajectory methods have become instrumental in uncovering deviations from normal Brownian motion of passively moving particles [9–22].

Classical diffusion patterns are sketched in the left panel of Fig. 1. Accordingly, one may observe free diffusion, leading to a linear growth with time of the second moment [Line 1 in Fig. 1]. Brownian motion may also be restricted (corrallated, confined). Confinement in a cell, for instance, could be due to the cell walls. In that case

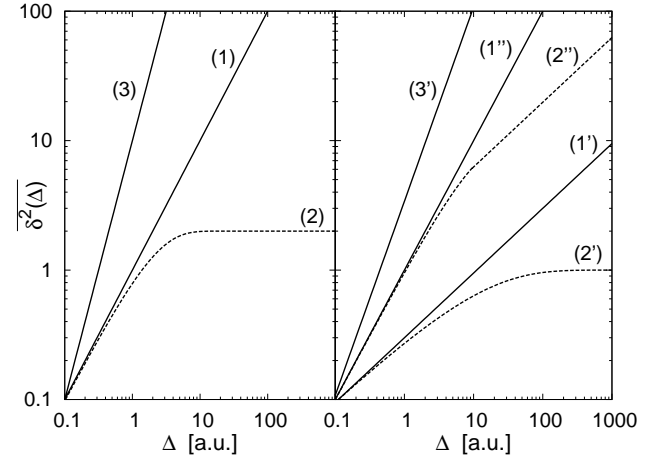


Figure 1: Diffusion modes of the time averaged mean squared displacement (2) as function of the lag time Δ . Left: Normal diffusion growing like $\overline{\delta^2} \simeq \Delta$ (1), restricted (confined) diffusion with a turnover from $\simeq \Delta$ to $\simeq \Delta^0$ (2), drift diffusion $\simeq \Delta^2$ (3). Right: Ergodic subdiffusion $\simeq \Delta^\alpha$ (1'), restricted ergodic subdiffusion turning over from $\simeq \Delta^\alpha$ to $\simeq \Delta^0$ (2'), non-ergodic subdiffusion $\simeq \Delta$ (1''), restricted non-ergodic subdiffusion turning over from $\simeq \Delta$ to $\simeq \Delta^{1-\alpha}$ (2''), superdiffusion $\Delta^{1+\alpha}$ (3'). Here, $0 < \alpha < 1$. Note the double-logarithmic scale.

the second moment initially grows linearly with time and eventually saturates to its thermal value equalling the second moment of the corresponding Boltzmann distribution [Line 2]. In the presence of a drift the second moment grows with the square of time [Line 3]. Such results are typical for simple fluids. In more complex environments, different patterns may be observed, as displayed on the right of Fig. 1. Here, subdiffusion may occur,

*Submitted to the special issue: Single Molecule Optical studies of Soft and Complex Matter

[†]Electronic address: metz@ph.tum.de

[‡]Electronic address: barkai@mail.biu.ac.il

for which the second moment grows slower than linearly with time [Line 1']. Restricted subdiffusion would depart from this behaviour to reach a plateau [Line 2']. Driven motion may lead to a superdiffusive power-law form of the second moment with an exponent between 1 and 2 [Line 3']. However, as we demonstrate below, subdiffusion may also be non-ergodic, and the associated time averaged second moment may grow *linearly* with time [Line 1'']. Similarly strange behaviour may be observed for restricted non-ergodic subdiffusion, which exhibits a *power-law* growth, not a saturation to a plateau [Line 2'']. Non-ergodic processes come along with a significant scatter between individual trajectories. This is an effect of the ageing nature of the process that persists for long measurement times. In the following we discuss in detail the behaviour of passive subdiffusive motion in terms of time and ensemble averages and address the peculiarities, that may arise for non-ergodic systems.

Non-ergodic behaviour of the above sense is indeed observed experimentally. Fig. 2 shows the time averaged mean squared displacement for lipid granules in a living fission yeast cell. The motion is recorded by indirect tracking in an optical tweezers setup. Initially the granule is located in the bottom of the laser trap potential such that the granule moves freely. Eventually the granule ventures away from the centre of the trap and experiences the Hookean trap force. As demonstrated in a detailed analysis the granule motion indeed exhibits weak ergodicity breaking, giving rise to the characteristic turnover from an initially linear scaling $\overline{\delta^2} \simeq \Delta$ with the lag time Δ , to the power-law regime $\overline{\delta^2} \simeq \Delta^{1-\alpha}$ [23]. Moreover a pronounced trajectory-to-trajectory scatter is observed, again typical for systems with weak ergodicity breaking.

Free diffusion is typically quantified in terms of the second moment. The mean squared displacement

$$\langle \mathbf{r}^2(t) \rangle \equiv \int \mathbf{r}^2 P(\mathbf{r}, t) d^3 \mathbf{r} \quad (1)$$

is obtained as the spatial average over the probability density function $P(\mathbf{r}, t)$ to find the particle at position \mathbf{r} at time t . The quantity (1) therefore corresponds to the ensemble averaged second moment of the particle position, denoted by angular brackets, $\langle \cdot \rangle$. In particular, the time t enters into Eq. (1) only as a parameter. Conversely, single particle trajectories $\mathbf{r}(t)$ are usually evaluated in terms of the time averaged mean squared displacement defined as

$$\overline{\delta^2(\Delta, T)} \equiv \frac{1}{T - \Delta} \int_0^{T-\Delta} (\mathbf{r}(t + \Delta) - \mathbf{r}(t))^2 dt, \quad (2)$$

where we use an overline $\overline{\cdot}$ to symbolise the time average. Here Δ is the so-called lag time constituting a time window swept along the time series, and T is the overall measurement time. The time averaged mean squared displacement thus compares the particle positions along the trajectory as separated by the time difference Δ .

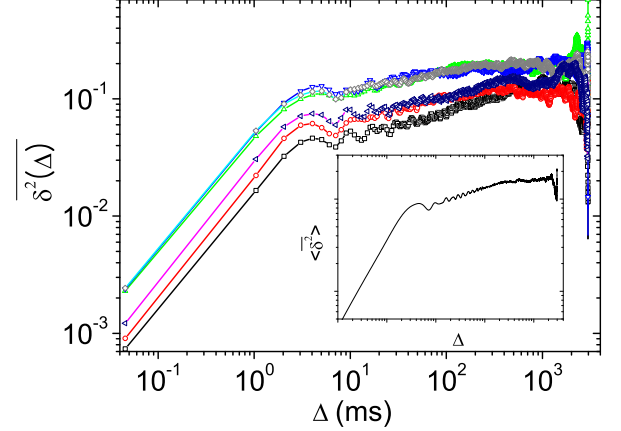


Figure 2: Time averaged mean squared displacement of lipid granule motion in fission yeast cell *S.pombe*, measured by optical tweezers. As function of the lag time Δ the initially linear scaling $\overline{\delta^2} \simeq \Delta$ turns over to the power-law regime $\overline{\delta^2} \simeq \Delta^{1-\alpha}$, induced by the restoring force exerted on the granules by the laser trap [23]. Note also the characteristic scatter between individual trajectories. Inset: Average behaviour of the shown trajectories. In both graphs the unit of $\overline{\delta^2(\Delta, T)}$ is Volt², i.e., the direct output voltage of the quadrant photodiode. The voltage is directly proportional to the distance from the centre of the laser trap.

In an ergodic system the time average of a certain quantity obtained from sufficiently long time series is equal to the corresponding ensemble mean [24, 25]. For instance, for the mean squared displacement ergodicity would imply

$$\lim_{T \rightarrow \infty} \overline{\delta^2(\Delta = t, T)} = \langle \mathbf{r}^2(t) \rangle. \quad (3)$$

Brownian motion is ergodic, as well as certain stationary processes leading to anomalous diffusion, such as fractional Brownian motion considered below. There exist, however, non-ergodic processes, which are intimately connected to ageing properties. In what follows we discuss two prominent models for anomalous diffusion, the stationary fractional Brownian motion and the ageing continuous time random walk, and analyse in detail the features of the associated time averaged mean squared displacement.

Generally, anomalous diffusion denotes deviations from the classical linear dependence of the mean squared displacement, $\langle \mathbf{r}^2(t) \rangle \simeq t$. Such anomalies include ultraslow diffusion of the form $\langle \mathbf{r}^2(t) \rangle \simeq \log^\beta t$ [26]. In contrast, anomalous diffusion processes may become faster than ballistic, for instance for systems with correlated jump lengths or in systems governed by generalised Langevin equations [27, 28]. Here we are interested in anomalous diffusion with power-law dependence on time [29],

$$\langle \mathbf{r}^2(t) \rangle \sim 2d \frac{K_\alpha}{\Gamma(1 + \alpha)} t^\alpha, \quad (4)$$

for which the anomalous diffusion exponent belongs to the subdiffusive range $0 < \alpha < 1$, such that the limit $\alpha = 1$ corresponds to Brownian motion. The proportionality factor K_α in Eq. (4) is the anomalous diffusion coefficient of physical dimension $\text{cm}^2/\text{sec}^\alpha$. The embedding spatial dimension is d , and Eq. (4) includes the complete Gamma function $\Gamma(z)$.

Subdiffusion of the form (4) with $0 < \alpha < 1$ occurs in the following biologically relevant systems. Fluorescently labelled mRNA in *E.coli* bacteria cells was observed to follow $\delta^2(\Delta, T) \simeq \Delta^\alpha$ with $\alpha \approx 0.7$ [9]. This result is consistent with more recent findings according to which free RNA tracers in living cells exhibit $\alpha \approx 0.8$, while DNA loci show $\alpha = 0.4$ [10]. Telomeres in the nucleus of mammalian cells were reported to follow anomalous diffusion with $\alpha \approx 0.3$ at shorter times and value $\alpha \approx 0.5$ at intermediate times, before a turnover to normal diffusion occurs [11]. Also larger tracer particles show anomalous diffusion, such as adeno-associated viruses of radius ≈ 15 nm in a cell with $\alpha = 0.5 \dots 0.9$ [12] and endogenous lipid granules, of typical size of few hundred nm with $\alpha \approx 0.75 \dots 0.85$ [13–15]. It should be noted that this subdiffusion observed by single particle tracking microscopy is consistent with results from other techniques, such as fluorescence correlation spectroscopy [17–20] or dynamic light scattering [21]. Subdiffusion of biopolymers larger than some 10 kD in living cells is due to molecular crowding, the excluded volume effect in the superdense cellular environment [30–32]. Larger tracer particles also experience subdiffusion due to interaction with the semiflexible cytoskeleton [22].

Knowledge of the time or ensemble averaged mean squared displacement of an anomalous diffusion process is insufficient to fully characterise the underlying stochastic mechanism, as the associated probability density $P(\mathbf{r}, t)$ is no longer necessarily Gaussian, and therefore no longer specified by the first and second moments, only [29]. This property is in contrast to the universal Gaussian nature of Brownian motion which is effected by the central limit theorem. At the same time the very nature of the anomalous diffusion process may result in decisively different behaviours for diffusional mixing and diffusion-limited reactions [33]. In biological cells this would imply significant differences for signalling and regulatory processes. For a better understanding of the dynamics in biological cells and other complex fluids knowledge of the underlying stochastic mechanism is therefore imperative.

Here we discuss the properties of continuous time random walk (CTRW) processes with diverging characteristic waiting time with respect to their time averaged behaviour, expanding on our earlier work [34–36]. We show that for free motion the lag time dependence of the time averaged mean squared displacement, $\delta^2(\Delta, T) \simeq \Delta$, is insensitive to the anomalous diffusion exponent α for CTRW processes. In contrast, for confined CTRW subdiffusion a universal scaling behaviour emerges, $\delta^2(\Delta, T) \simeq \Delta^{1-\alpha}$, with dynamic exponent $1-\alpha$ [curves (1') and (2'') in Fig. 1]. Subdiffusion governed

by fractional Brownian motion (FBM) leads to the scaling $\delta^2(\Delta, T) \simeq \Delta^\alpha$ of the time averaged mean squared displacement, turning over to a saturation plateau under confinement, $\delta^2(\Delta, T) \simeq \Delta^0$ [curves (1') and (2') in Fig. 1].

We particularly emphasise the irreproducible nature of the time averaged quantities and their associated scatter around the ensemble mean for CTRW subdiffusion processes. This randomness of the time averages is captured by the distribution function of the amplitude of the time average. We show that even for relatively short trajectories this distribution is a good characteristic for the underlying process. In contrast for FBM processes the scatter typical of many single particle experiments is not found in the long time limit.

In the remainder of this work, for simplicity we restrict the discussion to the one-dimensional case ($d = 1$). Generalisation to higher dimensions is straightforward. The article is structured as follows. We start with a brief introduction to CTRW and FBM. We then consider the cases of unbounded motion and confined anomalous diffusion in the subsequent two Sections. The distribution of the time averages will be presented thereafter. Finally, we discuss the velocity autocorrelation functions for subdiffusive CTRW and FBM processes, before presenting a concluding discussion.

II. ANOMALOUS DIFFUSION PROCESSES

Although both CTRW and FBM give rise to an ensemble averaged mean squared displacement of the form (1), they are fundamentally different processes, as outlined here. We note in passing that also in the random motion on a fractal support subdiffusion arises [37, 38]. We will not pursue this type of anomalous diffusion in the following.

A. Continuous time random walk

CTRW theory dates back to the work of Montroll and Weiss [39], and was championed in the analysis of charge carrier motion in amorphous semiconductors by Scher and Montroll [40]. CTRW has become a standard statistical tool to describe processes ranging from particle motion in actin networks [22] to the tracer motion in groundwater [41].

Each jump of a CTRW process is characterised by a random jump length and a random waiting time elapsing before the subsequent jump. At each jump the jump length and waiting time are chosen independently. For a subdiffusive process we assume that the variance of the jump lengths is given by a finite value $\langle \delta x^2 \rangle$, and we consider the unbiased case $\langle \delta x \rangle = 0$. On a lattice of spacing a , we would have $\langle \delta x^2 \rangle = a^2$. In contrast, the

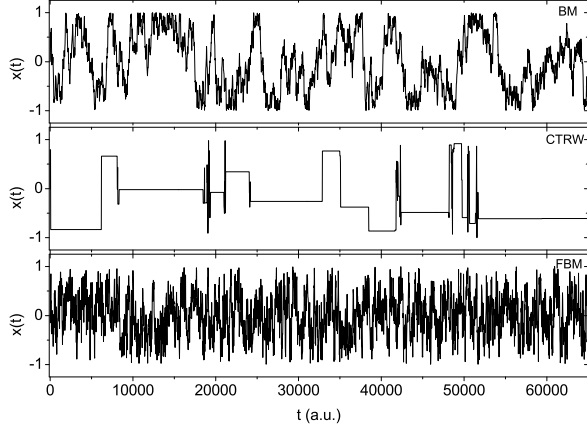


Figure 3: Time series $x(t)$ for Brownian motion (top), CTRW (middle), and FBM (bottom). The anomalous diffusion exponent for FBM and CTRW is $\alpha = 0.5$. For CTRW the stalling events are outstanding, while in the case of FBM strong anti-persistence occurs. Note that the stalling events and the anti-persistence are less pronounced for larger values of α . Typical experimental data include additional noise, such that the appearance of measured data will not display the ideal behaviour shown here.

waiting times τ are drawn from the probability density

$$\psi(\tau) \simeq \frac{\bar{\tau}^\alpha}{|\Gamma(-\alpha)|} \tau^{-1-\alpha} \quad (5)$$

for large τ , with $0 < \alpha < 1$. This form of ψ is scale-free, that is, the average waiting time $\langle \tau \rangle$ diverges, causing effects such as ageing [42, 43] and weak ergodicity breaking [44]. In Eq. (5), the quantity $\bar{\tau}$ is a scaling factor. The anomalous diffusion constant in this case becomes [29, 45]

$$K_\alpha = \frac{\langle \delta x^2 \rangle}{2\bar{\tau}^\alpha}. \quad (6)$$

The scale-freeness of $\psi(\tau)$ allows individual waiting times τ to become quite large. No matter how long a given time series is chosen, single τ values may become of the order of the length of the entire time span covered in the trajectory. An example is shown in Fig. 3: the stalling events with large waiting times τ are quite distinct. For values of the anomalous diffusion exponent α that are closer to 1 the stalling is less pronounced. Physically, the power-law form of the waiting time distribution $\psi(\tau)$ may be related to comb models [37] or random energy landscapes [42, 46]; for more details, compare Refs. [47–50].

B. Fractional Brownian motion

FBM is a Gaussian process with stationary increments. Its position is defined in terms of the Langevin equation

$$\frac{dx(t)}{dt} = \xi(t), \quad (7)$$

or, alternatively,

$$x(t) = \int_0^t \xi(t') dt'. \quad (8)$$

The motion is driven by stationary, fractional Gaussian noise $\xi(t)$ with zero mean $\langle \xi(t) \rangle$ and long-ranged noise correlation [51]

$$\begin{aligned} \langle \xi(t_1) \xi(t_2) \rangle &= \alpha K_\alpha^* (\alpha - 1) |t_1 - t_2|^{\alpha-2} \\ &\quad + 2\alpha K_\alpha^* |t_1 - t_2|^{\alpha-1} \delta(t_1 - t_2), \end{aligned} \quad (9)$$

contrasting the uncorrelated noise for normal diffusion $\alpha = 1$: $\langle \xi(t_1) \xi(t_2) \rangle = 2K_1 \delta(t_1 - t_2)$. In Eq. (9) the anomalous diffusion exponent is connected to the traditionally used Hurst exponent by $H = \alpha/2$, and we introduce the abbreviation $K_\alpha^* = K_\alpha / \Gamma(1 + \alpha)$ for consistency with standard FBM notation. For subdiffusion the fractional Gaussian noise is anticorrelated, decaying like $\langle \xi(t_1) \xi(t_2) \rangle \sim -K_\alpha^* \alpha |\alpha - 1| |t_1 - t_2|^{\alpha-2}$. This implies that a given step is likely to go into the direction opposite to the previous step. The corresponding oscillating behaviour is seen in Fig. 3. The position autocorrelation function of FBM becomes

$$\langle x(t_1) x(t_2) \rangle = K_\alpha^* (t_1^\alpha + t_2^\alpha - |t_1 - t_2|^\alpha), \quad (10)$$

so that at equal times $t_1 = t_2$ we recover the mean squared displacement (4).

If the fractional Gaussian noise is not considered external, but the validity of the fluctuation-dissipation theorem is imposed, one obtains the generalised Langevin equation (GLE) [52],

$$m \frac{d^2 x(t)}{dt^2} = -\bar{\gamma} \int_0^t (t - t')^{\beta-2} \frac{dx}{dt'} dt' + \eta \xi(t), \quad (11)$$

where we write β instead of the exponent α in Eq. (9). In the GLE (11), we defined the coupling coefficient $\eta = \sqrt{k_B \mathcal{T} \bar{\gamma} / [\beta K_\beta^* (\beta - 1)]}$ according to the fluctuation-dissipation theorem, where k_B is the Boltzmann constant and \mathcal{T} the absolute temperature. In what follows we only consider the overdamped limit, in which the inertia term $m d^2 x(t) / dt^2$ can be neglected. The GLE then gives rise to the form

$$\langle x^2(t) \rangle \simeq t^{2-\beta} \quad (12)$$

of the mean squared displacement. In contrast to FBM, that is, the GLE leads to subdiffusion for persistent noise with $1 < \beta < 2$, while $0 < \beta < 1$ yields superdiffusion.

FBM and the related GLE are used to describe processes such as long term storage capacity of water reservoirs [53], climate fluctuations [54], economical market dynamics [55], single file diffusion [56], and elastic models [57]. Motion of this type has also been associated with the relative motion of aminoacids in proteins [58], and the free diffusion of biopolymers under molecular crowding conditions [10, 19, 59].

III. FREE ANOMALOUS DIFFUSION

Let us begin with considering anomalous diffusion on an infinite domain and without drift. To find an analytical expression for the time averaged mean squared displacement (2) we note that even a Brownian process recorded over a finite time span T will show fluctuations in the number of jumps performed during T . To average out these trajectory-to-trajectory fluctuations we introduce the ensemble mean,

$$\langle \overline{\delta^2(\Delta, T)} \rangle = \frac{1}{T - \Delta} \int_0^{T-\Delta} \left\langle \left(x(t + \Delta) - x(t) \right)^2 \right\rangle dt. \quad (13)$$

We can then express the integrand in terms of the variance of the jump lengths, $\langle \delta x^2 \rangle$, and the average number of jumps $n(t, t + \Delta)$ in the time interval $(t, t + \Delta)$, as follows:

$$\left\langle \left(x(t + \Delta) - x(t) \right)^2 \right\rangle = \langle \delta x^2 \rangle n(t, t + \Delta). \quad (14)$$

For a regular random walk on average every jump occurs after the waiting time $\langle \tau \rangle$. Thus $n(t, t + \Delta) = \Delta / \langle \tau \rangle$, and

$$\langle \overline{\delta^2(\Delta, T)} \rangle = 2K_1 \Delta, \quad (15)$$

where we defined the diffusion constant $K_1 = \langle \delta x^2 \rangle / [2\langle \tau \rangle]$. In the Brownian limit the time averaged mean squared displacement (15) in terms of the lag time Δ takes on exactly the same form as the ensemble averaged mean squared displacement (1) as function of time t . This is not surprising, as Brownian motion is an ergodic process. For sufficient duration T of the time records any time average converges to the corresponding ensemble average, and thus the ensemble average in expression (13) is no longer necessary.

A. Continuous time random walk

The number of jumps of a CTRW process with waiting time distribution of the form (5) on average grows sublinearly with time, $n(0, t) \sim t^\alpha / [\bar{\tau}^\alpha \Gamma(1 + \alpha)]$ [47]. This time evolution translates into the mean squared displacement (1) with the anomalous diffusion coefficient (6). Combining the time dependence of $n(0, t)$ for CTRW subdiffusion

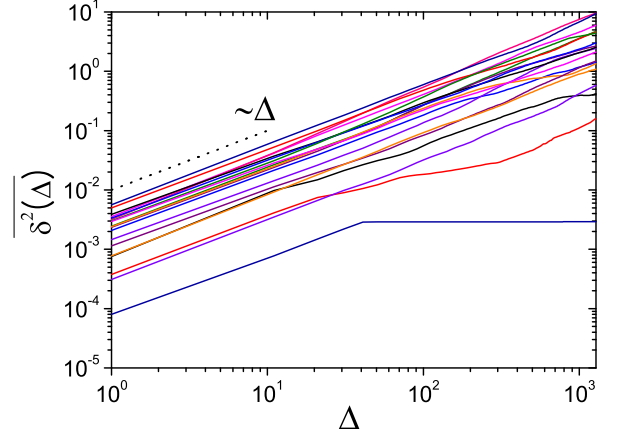


Figure 4: Time averaged mean squared displacement for unconfined CTRW motion with $\alpha = 0.5$, shown for 20 individual trajectories. The overall measurement time is $T = 10^5$ (a.u.). Note the local changes of the slope in the trajectories as well as the complete stalling in the lowest curve, all bearing witness to the scale-free nature of the underlying waiting time distribution $\psi(\tau) \simeq \bar{\tau}^\alpha / \tau^{1+\alpha}$.

with the definition (13) we obtain the following result for the time averaged mean squared displacement,

$$\langle \overline{\delta^2(\Delta, T)} \rangle \sim 2K_\alpha \frac{\Delta}{T^{1-\alpha}} \quad (16)$$

in the limit $\Delta \ll T$ [34, 60]. This follows from expansion of the relation $n(t, t + \Delta) = n(0, t + \Delta) - n(0, t)$. The noteworthy feature of this result is that the linear lag time dependence of normal diffusion remains completely unaffected by the anomalous nature of the stochastic process. Only the dependence on the overall measurement time T witnesses the underlying subdiffusion. Eq. (16) can be understood if we notice that for normal diffusion we have $\delta^2(\Delta, T) \simeq \Delta / \langle \tau \rangle$ [since according to Einstein $K_1 \propto 1 / \langle \tau \rangle$] where $\langle \tau \rangle$ is the mean time between jump events. Now, for the subdiffusive case $\langle \tau \rangle$ diverges and must be replaced by $\int_0^T \psi(\tau) \tau d\tau \propto T^{1-\alpha}$, which explains the term $\delta^2 \propto \Delta / T^{1-\alpha}$. Fig. 4 shows 20 trajectories of a CTRW process with $\alpha = 0.5$, displaying the general trend $\overline{\delta^2}(\Delta, T) \simeq \Delta$.

Rewriting the result (16) in the form

$$\langle \overline{\delta^2(\Delta, T)} \rangle \sim 2\bar{K}(T) \Delta \quad (17)$$

we see that the effective diffusion coefficient $\bar{K}(T)$ decays as function of the measurement time T . The longer the system evolves after its initial preparation, the less mobile it appears, consistent with the ageing property of CTRW subdiffusion. For instance, in the picture of the trapping events, in the course of time deeper and deeper traps may be encountered by the diffusing particle, such

that it gets more and more stuck. This increasing immobility is mirrored in the form $\bar{K}(T)$. Note that Eqs. (16) and (17) suggest that from measuring the Δ dependence of an anomalous diffusion process one might draw the erroneous conclusion that normal diffusion were observed.

The disparity between the time averaged mean squared displacement (16) and its ensemble averaged counterpart (4) demonstrates the weak ergodicity breaking characteristic of a process with diverging time scale [42, 44]. Single or few, long waiting times are also responsible for the pronounced deviations between individual realisations shown in Fig. 4. This apparent irreproducibility of the time averaged mean squared displacement is again intimately coupled to the weak ergodicity breaking nature of the CTRW subdiffusion process. We will discuss this feature more quantitatively in terms of the distribution $\phi_\alpha(\xi)$ as function of the relative deviation $\xi = \bar{\delta}^2 / \langle \bar{\delta}^2 \rangle$ of the time averaged mean squared displacement around its ensemble mean in Section V.

B. Fractional Brownian motion

In contrast to the above behaviour of CTRW subdiffusion processes, FBM is ergodic. Indeed, by help of the position autocorrelation (10) the time averaged mean squared displacement (13) becomes [61]

$$\langle \bar{\delta}^2(\Delta, T) \rangle = 2K_\alpha^* \Delta^\alpha, \quad (18)$$

exactly matching the ensemble averaged mean squared displacement, $\langle x^2(t) \rangle = 2K_\alpha^* t^\alpha$. However, ergodicity is reached algebraically slowly [61], see also below. In Fig. 5 the comparatively minute scatter between individual trajectories supports the ergodic behaviour of FBM processes. The somewhat larger deviations at longer lag times are due to worsening statistics when $\Delta \rightarrow T$.

IV. CONFINED ANOMALOUS DIFFUSION

Since the motion of tracer particles is typically confined, for example, by the cell walls or internal membranes, we now consider the important case of anomalous diffusion in a bounded domain.

In a finite interval $[-L, L]$ the mean squared displacement of a Brownian particle initially released well away from the boundaries will grow linearly in time and eventually turn over to a stationary plateau of magnitude $\langle x^2 \rangle_{\text{st}} = L^2/3$. Similarly, if the particle evolves in the confinement of an external harmonic potential of the form $V(x) = \frac{1}{2}m\omega^2 x^2$, the thermal value $\langle x^2 \rangle_{\text{th}} = k_B T / [m\omega^2]$ will eventually be attained.

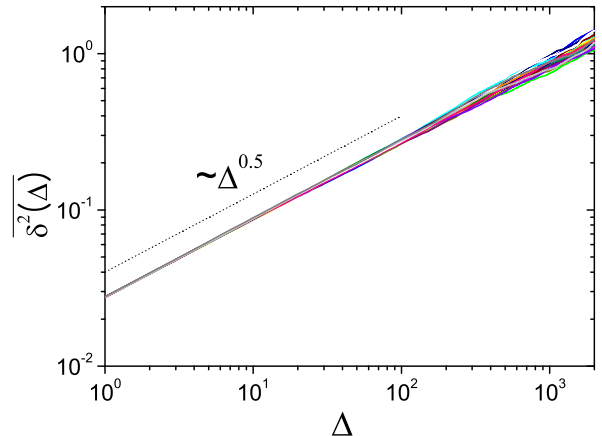


Figure 5: Time averaged mean squared displacement for unconfined FBM with $\alpha = 0.5$. The scatter between individual trajectories is minute, mirroring the ergodicity of this process.

A. Continuous time random walk

How is this behaviour modified for a CTRW subdiffusion process? Under the influence of an arbitrary external potential $V(x) = -\int^x F(x')dx'$ defining the force $F(x)$, CTRW subdiffusion can be described by the fractional Fokker-Planck equation [29, 45], or, equivalently, in terms of the following coupled Langevin equations [62]:

$$\frac{dx(s)}{ds} = \frac{K}{k_B T} F(x) + \eta(s) \quad (19a)$$

$$\frac{dt(s)}{ds} = \omega(s). \quad (19b)$$

Here the position x is expressed in terms of the parameter s (the internal time), and driven by the white Gaussian noise $\eta(s)$. Thus, Eq. (19a) defines standard Brownian motion $x(s)$, where K is the diffusivity for the normal diffusion process in internal time s . Laboratory time t is introduced by the so-called subordination through the process $\omega(s)$, given by the probability density function [29]

$$p_t(s) = \frac{1}{\alpha} \left(\frac{K_\alpha}{K} \right)^{1/\alpha} \frac{t}{s^{1+1/\alpha}} l_\alpha \left(\left[\frac{K_\alpha}{K} \right]^{1/\alpha} \frac{t}{s^{1+1/\alpha}} \right), \quad (20)$$

where $l_\alpha(z)$ is a one-sided Lévy stable probability density with Laplace transform $\int_0^\infty l_\alpha(z) \exp(-uz) dz = \exp(-u^\alpha)$. Thus, Eq. (19b) transforms the Brownian process $x(s)$ with diffusivity K into the subdiffusive motion with generalised diffusivity K_α . On the basis of this scheme, the ensemble averaged position-position correlation in an arbitrary confining potential $V(x)$ becomes

$$\langle x(t_1)x(t_2) \rangle = \left(\langle x^2 \rangle_B - \langle x \rangle_B^2 \right) \frac{B(t_1/t_2, \alpha, 1-\alpha)}{\Gamma(\alpha)\Gamma(1-\alpha)} + \langle x \rangle_B^2, \quad (21)$$

valid in the limit $t_2 \geq t_1 \gg (1/[K_\alpha \lambda_1])^{1/\alpha}$, where λ_1 is the smallest non-zero eigenvalue of the corresponding Fokker-Planck operator [35]. Eq. (21) demonstrates that, despite the confinement, the process is non-stationary. In result (21) we used the incomplete Beta function

$$B(t_1/t_2, \alpha, 1 - \alpha) \equiv \int_0^{t_1/t_2} z^{\alpha-1} (1-z)^{-\alpha} dz \quad (22)$$

and defined the first and second Boltzmann moments, whose general definition is

$$\langle x^n \rangle_B = \frac{1}{\mathcal{Z}} \int_{-\infty}^{\infty} x^n \exp\left(-\frac{V(x)}{k_B T}\right) dx. \quad (23)$$

The partition function reads

$$\mathcal{Z} = \int_{-\infty}^{\infty} \exp\left(-\frac{V(x)}{k_B T}\right) dx. \quad (24)$$

At large time separation, $t_2 \gg t_1$, the position autocorrelation decays algebraically,

$$\langle x(t_1)x(t_2) \rangle \sim \left(\langle x^2 \rangle_B - \langle x \rangle_B^2 \right) \frac{(t_1/t_2)^\alpha}{\alpha \Gamma(1+\alpha) \Gamma(1-\alpha)} + \langle x \rangle_B^2, \quad (25)$$

towards the value $\langle x \rangle_B^2$. The corresponding limiting behaviour of the incomplete Beta function reads

$$\frac{B(t/(t+\Delta), \alpha, 1-\alpha)}{\Gamma(\alpha)\Gamma(1-\alpha)} \sim 1 - \frac{\sin(\pi\alpha)}{(1-\alpha)\pi} \left(\frac{\Delta}{t}\right)^{1-\alpha}. \quad (26)$$

Inserting expression (21) into the definition of the time averaged mean squared displacement (13) we obtain [35]

$$\begin{aligned} \langle \overline{\delta^2(\Delta, T)} \rangle &= \frac{1}{T-\Delta} \int_0^{T-\Delta} \left[\langle x(t+\Delta)x(t+\Delta) \rangle \right. \\ &\quad \left. + \langle x(t)x(t) \rangle - 2\langle x(t+\Delta)x(t) \rangle \right] dt. \end{aligned} \quad (27)$$

Then, with relation (26) we arrive at the scaling behaviour

$$\langle \overline{\delta^2(\Delta, T)} \rangle \sim \left(\langle x^2 \rangle_B - \langle x \rangle_B^2 \right) \frac{2 \sin(\pi\alpha)}{(1-\alpha)\pi\alpha} \left(\frac{\Delta}{T}\right)^{1-\alpha}, \quad (28)$$

valid in the limits $\Delta/T \ll 1$ and $\Delta \gg (1/[K_\alpha \lambda_1])^{1/\alpha}$. Result (28) is quite remarkable: instead of the naively assumed saturation toward the stationary plateau a power-law growth $\langle \overline{\delta^2(\Delta, T)} \rangle \sim (\Delta/T)^{1-\alpha}$ is observed. Only when the lag time Δ approaches the overall measurement time T the singularity in expression (13) causes a dip toward the plateau of the ensemble averaged mean squared displacement. Additionally Eqs. (21) and (28) are universal in the sense that the exact form of the confining potential solely enters into the prefactor through the first two moments of the Boltzmann distribution corresponding to the confining potential $V(x)$. We note that the

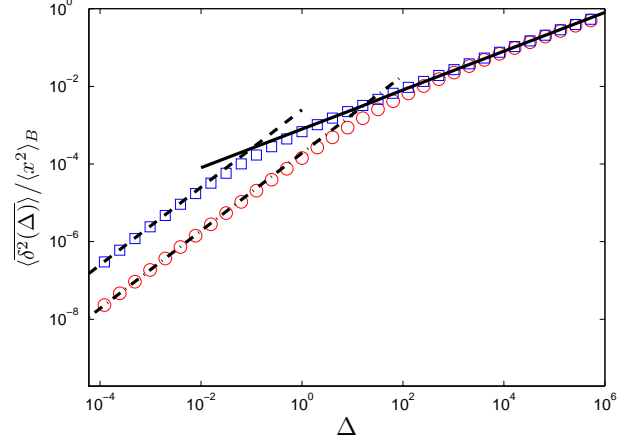


Figure 6: Simulated behaviour of $\langle \overline{\delta^2(\Delta)} \rangle$ for an harmonic binding potential $V(x) = 2x^2$ (\square) and a particle in a box of length 2 (\circ), with $\alpha = 1/2$, measurement time $T = 10^7$ (a.u.), $k_B T = 0.1$, and $K_{0.5} = 0.0892$. Without fitting, the lines show the analytic results for the transition from $\simeq \Delta^1$ for short lag times according to Eq. (16) (--- and - · -) to $\simeq \Delta^{1-\alpha}$ for long lag times, Eq. (28) (—). For long Δ , $\langle \overline{\delta^2(\Delta)} \rangle / \langle x^2 \rangle_B$ exhibits universal behaviour, in the sense that the curve does not depend on the external field.

asymptotic scaling $\simeq (\Delta/T)^{1-\alpha}$ is consistent with the numerical analysis presented in Ref. [63].

Fig. 6 depicts the ensemble mean of the time averaged mean squared displacement (13) for two types of confinement, an harmonic potential and a box potential. The particle is initially placed at the bottom of the potential well and in the middle of the box potential, respectively. This is why at short lag times the particle exhibits the linear scaling $\langle \overline{\delta^2(\Delta, T)} \rangle \simeq \Delta$ typical for unconfined motion, before turning over to the confinement-induced scaling $\simeq \Delta^{1-\alpha}$. Note that this plot is fit-free, i.e., the theoretically calculated asymptotic behaviours nicely fall on top of the simulations results.

As shown in Fig. 7 individual trajectories still exhibit the pronounced scatter typical for CTRW subdiffusion. Visually the scatter does not change between the unbiased initial motion and the confinement-dominated part of the process. This is due to the fact that the scatter is caused by the scale-freeness of the waiting times. In our process waiting times and jump lengths are decoupled, corresponding to the subordination property of CTRW subdiffusion [29].

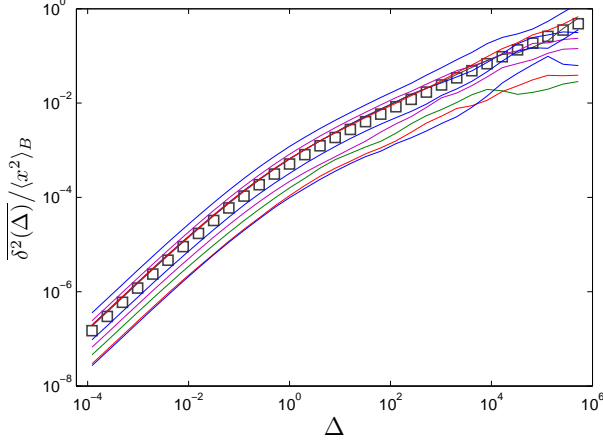


Figure 7: Scatter between individual trajectories in the harmonic potential $V(x) = 2x^2$. The extent of the deviations between the trajectories does not change qualitatively between the initial unbiased motion and the later confinement-dominated regime. The squares (\square) represent simulations results for the ensemble average $\langle \overline{\delta^2(\Delta, T)} \rangle$. Same parameters as in Fig. 6.

B. Continuous time random walk with waiting time cutoff

What happens if we introduce a cutoff in the power-law of the waiting time distribution of the form

$$\psi(\tau) = \frac{d}{d\tau} \left[1 - \frac{\bar{\tau}^\alpha}{(\bar{\tau} + \tau)^\alpha} \exp\left(-\tau/\tau^*\right) \right], \quad (29)$$

in which a characteristic time scale τ^* is introduced, terminating the power-law scaling? For the waiting time density (29) the characteristic waiting time $\int_0^\infty \tau \psi(\tau) d\tau$ becomes finite. At sufficiently short times one would expect this process to still exhibit the features of CTRW subdiffusion, while at times $\tau \gg \tau^*$ the process should converge to regular Brownian motion with a Gaussian propagator. In Fig. 8 we demonstrate that for a suitable choice of the cutoff time τ^* the behaviour of the time averaged mean squared displacement $\overline{\delta^2(\Delta, T)}$ under confinement preserves the characteristic non-ergodic features of CTRW subdiffusion, i.e., the turnover from the initial scaling $\simeq \Delta$ to the confinement-dominated scaling $\Delta^{1-\alpha}$. Below we will show that at the same time the distribution of the time average around its ensemble mean is significantly altered.

C. Fractional Brownian motion

Ergodicity remains unaffected for FBM, that is confined to an interval of size $[-L, L]$. Namely, convergence of $\overline{\delta^2(\Delta, T)}$ is observed toward the stationary value

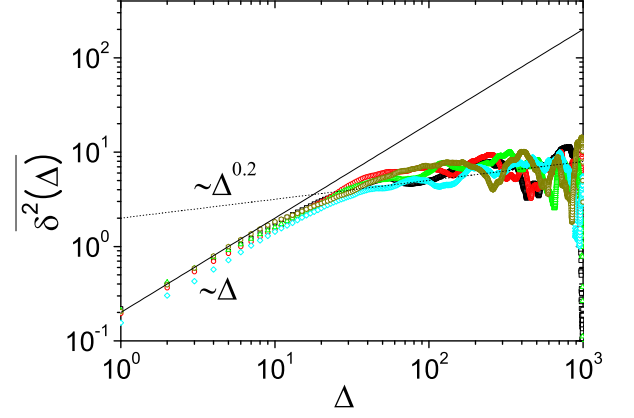


Figure 8: CTRW subdiffusion for a waiting time with exponential cutoff, Eq. (29), in the box $[-3, 3]$ with reflecting boundary conditions. The generic behaviour of initial and final scaling, $\overline{\delta^2(\Delta, T)} \simeq \Delta$ and $\simeq \Delta^{1-\alpha}$ remains unaltered. We chose $\alpha = 0.8$, $\bar{\tau} = 1$, $\tau^* = 20$ and overall measurement time $T = 1000$ (a.u.).

$\langle x^2 \rangle_{\text{st}} = L^2/3$ [64]. For FBM under the influence of an harmonic potential $V(x) = \frac{1}{2}m\omega^2 x^2$ the position-position correlation can be calculated exactly [65]. Inserting into the ensemble mean (13) of the time averaged mean squared displacement one can show that the initial behaviour $\langle x^2(t) \rangle \simeq t^\alpha$ turns over to the stationary value $\langle x^2 \rangle_{\text{st}} = \Gamma(\alpha + 1)k_B T / [m\omega^2]$. In general, the time averaged mean squared displacement for confined FBM converges to a constant:

$$\langle \overline{\delta^2(\Delta, T)} \rangle \sim \text{const.} \quad (30)$$

V. FLUCTUATIONS OF THE TIME AVERAGE AND ERGODICITY BREAKING PARAMETER

The deviations of the time averaged mean squared displacement $\delta^2(\Delta, T)$ between individual trajectories can be quantified in terms of the probability density function $\phi_\alpha(\xi)$ of the dimensionless ratio

$$\xi \equiv \frac{\overline{\delta^2(\Delta, T)}}{\langle \overline{\delta^2(\Delta, T)} \rangle} \quad (31)$$

of the time averaged mean squared displacement over its ensemble mean. For an ergodic process this distribution is necessarily sharp,

$$\phi_{\text{erg}}(\xi) = \delta(\xi - 1), \quad (32)$$

for long measurement time T . Deviations from this form are expected for non-ergodic processes such as CTRW subdiffusion, but also for relatively short trajectories. We

here address both effects and demonstrate that the distribution $\phi_\alpha(\xi)$ is a quite reliable means to distinguish different stochastic processes even when the recorded time series are fairly short.

A. Continuous time random walk

For CTRW subdiffusion with power-law waiting time distribution (5) the distribution assumes the form [34, 66]

$$\phi_\alpha(\xi) = \frac{\Gamma(1+\alpha)^{1/\alpha}}{\alpha \xi^{1+1/\alpha}} l_\alpha \left(\frac{\Gamma(1+\alpha)^{1/\alpha}}{\xi^{1/\alpha}} \right) \quad (33)$$

for $T \rightarrow \infty$, where $l_\alpha(z)$ is again a one-sided Lévy stable distribution, whose Laplace transform is $\mathcal{L}\{l_\alpha(z)\} = \exp(-u^\alpha)$. Special cases include the Brownian limit (32) for $\alpha = 1$ and the Gaussian shape

$$\phi_{1/2}(\xi) = \frac{2}{\pi} \exp\left(-\frac{\xi^2}{\pi}\right) \quad (34)$$

for $\alpha = 1/2$. In fact, we observe an exponentially fast decay of $\phi_\alpha(\xi)$ with large ξ for all $0 < \alpha < 1$, compare Appendix A.

For short trajectories the basic shape of the distribution $\phi_\alpha(\xi)$ is surprisingly well preserved [67]. This is demonstrated in Fig. 9, in which the characteristic asymmetric shape with respect to the ergodic value $\xi = 1$ for the case $\alpha = 0.5$ is reproduced for a process with $T = 128$, even for a lag time as long as $\Delta = 100$. No significant dependence on the confinement is observed. Also for larger values of α the finite value for small ξ is similarly reproduced for short trajectories [67], pointing at the quite remarkably reliability on the shape of the scatter distribution $\phi_\alpha(\xi)$ for CTRW subdiffusion. As we show below, the distribution for FBM processes with its zero value at $\xi = 0$ can be clearly distinguished from the CTRW form.

A useful parameter to quantify the violation of ergodicity is the ergodicity breaking parameter [34]

$$\text{EB} = \lim_{T \rightarrow \infty} \frac{\left\langle \left(\overline{\delta^2} \right)^2 \right\rangle - \left\langle \overline{\delta^2} \right\rangle^2}{\left\langle \overline{\delta^2} \right\rangle^2} = \frac{2\Gamma(1+\alpha)^2}{\Gamma(1+2\alpha)} - 1 \quad (35)$$

EB varies from $\text{EB} = 1$ for $\alpha \rightarrow 0$ monotonically to $\text{EB} = 0$ in the Brownian limit $\alpha = 1$. For the special case $\alpha = 1/2$ one finds $\text{EB} = \pi/2 - 1 \approx 0.57$, while for $\alpha = 0.75$, $\text{EB} \approx 0.27$.

B. Continuous time random walk with waiting time cutoff

The scatter distribution is sensitive to few extreme events. When these are lacking, the distribution should be significantly different from the form discussed for CTRW subdiffusion with diverging characteristic time

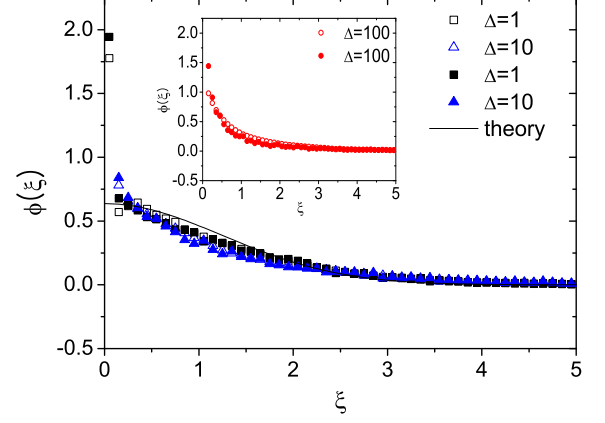


Figure 9: Distribution $\phi_\alpha(\xi)$ of the time averaged mean squared displacement, with $\xi = \overline{\delta^2} / \langle \overline{\delta^2} \rangle$ for a CTRW process with $\alpha = 0.5$, $\overline{\tau} = 1$, and $T = 128$ (a.u.). The filled and open symbols, respectively, represent the unconfined case and confined motion on the interval $[-2, 2]$. We see quite good agreement with the expected Gaussian limiting distribution of the scatter, Eq. (34), centred around $\xi = 0$. In the inset we show the case for the largest measured lag time, $\Delta = 100$, also in good agreement with the predicted shape of the distribution.

scale. Indeed, as shown in Fig. 10 for the cutoff waiting time distribution defined through Eq. (29), $\phi_\alpha(\xi)$ drops down to zero around $\xi = 0$ and assumes an almost Gaussian shape around the ergodic value $\xi = 1$. Note that the simulations were performed with the same parameters as for Fig. 8, in which the breaking of ergodicity still persists, despite the cutoff. This demonstrates that different quantities have different sensitivity to the cutoff.

C. Fractional Brownian motion

FBM is based on long-ranged correlations. However, we can obtain an approximate expression for the scatter distribution [67]

$$\phi(\xi) \approx \sqrt{\frac{T-\Delta}{4\pi\tau^\dagger}} \exp\left(-\frac{(\xi-1)^2(T-\Delta)}{4\tau^\dagger}\right). \quad (36)$$

where τ^\dagger is an intrinsic time scale. Expression (36) is valid for sufficiently small lag times Δ , for which the correlations are neglected [67]. Note that this distribution is independent of α and centred around the ergodic value $\xi = 1$. In particular, in the long measurement time limit $T \rightarrow \infty$, the distribution converges to the sharp form $\phi(\xi) = \delta(\xi - 1)$. Also this behaviour is surprisingly well preserved for short trajectories, as demonstrated in Fig. 11.

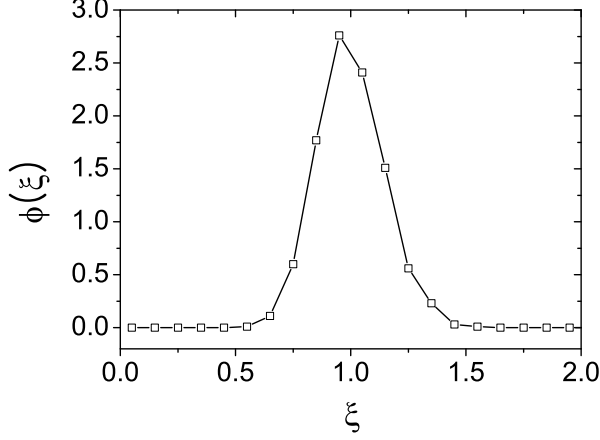


Figure 10: Scatter distribution $\phi_\alpha(\xi)$ for CTRW subdiffusion with cutoff, as defined in Eq. (29). The observed form is clearly different from the much more asymmetric shape in Fig. 9. The value of $\phi_\alpha(\xi)$ reaches zero for small values of ξ . An almost Gaussian shape centred around the ergodic value $\xi = 1$ is observed. Same parameters as in Fig. 8.

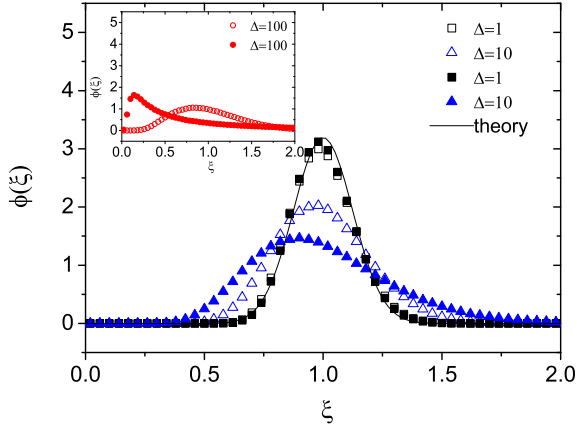


Figure 11: Scatter distribution $\phi(\xi)$ of the time averaged mean squared displacement, with $\xi = \overline{\delta^2} / \langle \delta^2 \rangle$ for FBM subdiffusion with $\alpha = 0.5$ and $T = 128$ (a.u.). The filled and open symbols, respectively, represent the cases for unconfined and confined motion. For small values of the lag time Δ we see quite good agreement with the expected Gaussian limiting distribution of the scatter, Eq. (36), that is centred around $\xi = 1$. For larger values of Δ deviations are observed, however, even for $\Delta = 100$ the value around $\xi = 0$ is consistently zero. A similar behaviour is found for larger values of α [67]. Note that when $T \rightarrow \infty$ the process is ergodic and $\phi(\xi)$ approaches a δ function.

For FBM one can define a quantity similar to the ergodicity breaking parameter (35). Namely, without taking the long measurement time limit, we obtain the normalised variance of the time averaged mean squared displacement

$$V = \frac{\langle (\overline{\delta^2}(\Delta, T))^2 \rangle - \langle \overline{\delta^2}(\Delta, T) \rangle^2}{\langle \overline{\delta^2}(\Delta, T) \rangle^2}. \quad (37)$$

It turns out that the convergence to ergodicity is algebraically slow, and for subdiffusion $0 < \alpha < 1$ one obtains a decay, which is inversely proportional to T [61]:

$$V \sim k(\alpha) \frac{\Delta}{T}. \quad (38)$$

The coefficient $k(\alpha)$ here is defined as [61]

$$k(\alpha) = \int_0^\infty \left((t+1)^\alpha + |t-1|^\alpha - 2t^\alpha \right) dt. \quad (39)$$

It increases continuously from zero at $\alpha = 0$ to $k(1) = 4/3$.

The quantity V is connected to the probability density (36) by $V = 2\tau^\dagger / (T - \Delta) \sim 2\tau^\dagger / T$, obtained from approximating that the values of ξ may range in the interval $(-\infty, \infty)$, which appears reasonable given the sharp decay of $\phi(\xi)$ to 0 at $\xi = 0$ for FBM. Apart from the fact that V explicitly depends on α while the approximation leading to Eq. (36) loses the α dependence, both quantities decay $\sim 1/T$, and the internal time scale τ^\dagger takes on a role similar to the lag time Δ .

VI. VELOCITY AUTOCORRELATION FUNCTIONS

A typical quantity accessible from experimental data is the velocity autocorrelation function, which is defined through

$$C_v^{(\epsilon)}(\tau) = \frac{1}{\epsilon^2} \langle (x(\tau + \epsilon) - x(\tau)) (x(\epsilon) - x(0)) \rangle. \quad (40)$$

Here the velocity is defined as the difference quotient $v(\tau) = \epsilon^{-1}[x(\tau + \epsilon) - x(\tau)]$. The velocity autocorrelation (40) was suggested as a tool to distinguish between different subdiffusion models [10]. We show here that for confined processes the shape of the velocity autocorrelation function does not allow for a significant distinction between subdiffusive CTRW and FBM. Note that the calculation of $C_v^{(\epsilon)}(\tau)$ amounts to determine four two-point correlation functions of the type $\langle x(t_1)x(t_2) \rangle$.

A. Continuous time random walk

For unbounded CTRW process starting with initial condition $x(0) = 0$, the position correlation function is

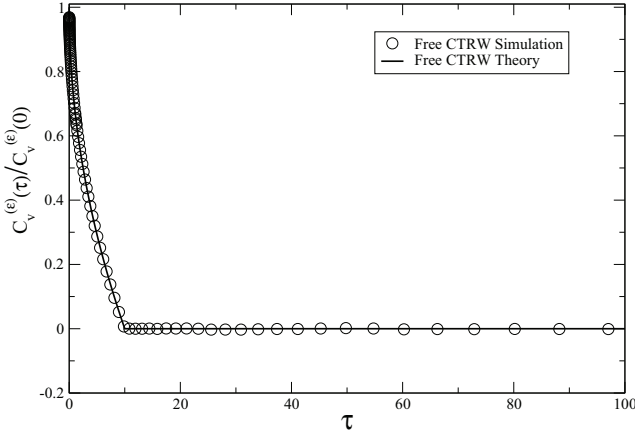


Figure 12: Normalised velocity autocorrelation function $C_v^{(\epsilon)}(\tau)$ for an unconfined CTRW process with $\alpha = 0.5$. The simulations (\circ) were performed for time 10000 (a.u) with $\epsilon = 10$ (a.u). The theoretical behaviour ($—$) is given by Eq. (42).

given by the following expression [68],

$$\langle x(t_1)x(t_2) \rangle = \frac{2K_\alpha}{\Gamma(1+\alpha)} [\min\{t_1, t_2\}]^\alpha. \quad (41)$$

This result for free CTRW is due to the fact that the jump lengths in the interval (t_1, t_2) for $t_2 > t_1$ have zero mean. With Eq. (41) we find

$$\frac{C_v^{(\epsilon)}(\tau)}{C_v^{(\epsilon)}(0)} = \begin{cases} \frac{\epsilon^\alpha - \tau^\alpha}{\epsilon^\alpha} & \tau \leq \epsilon \\ 0 & \tau \geq \epsilon \end{cases} \quad (42)$$

The velocity autocorrelation function for an unbounded CTRW process does not yield negative values due to the absence of correlations for different jumps. In this case the velocity autocorrelations can be easily distinguished from the behaviour of FBM processes, see below. Note that $C_v^{(\epsilon)}(\tau)$ in Eq. (42) is non-analytic at $\tau = \epsilon$, an observation that is confirmed in simulations. The behaviour of the velocity autocorrelations for CTRW subdiffusion are displayed in Fig. 12.

For a confined CTRW process the situation is quite different. To explore the behaviour of the corresponding velocity autocorrelation function we use the general result for the correlation function of confined CTRW, Eq. (21). For simplicity we assume a symmetric potential such that $\langle x \rangle_B = 0$. With the initial condition $x(0) = 0$ we obtain

$$\frac{C_v^{(\epsilon)}(\tau)}{C_v^{(\epsilon)}(0)} = \frac{1}{\Gamma(\alpha)\Gamma(1-\alpha)} \times \begin{cases} B\left(\frac{\epsilon}{\epsilon+\tau}, \alpha, 1-\alpha\right) - B\left(\frac{\tau}{\epsilon}, \alpha, 1-\alpha\right) & \epsilon \geq \tau \\ B\left(\frac{\epsilon}{\epsilon+\tau}, \alpha, 1-\alpha\right) - B\left(\frac{\epsilon}{\tau}, \alpha, 1-\alpha\right) & \epsilon \leq \tau \end{cases}. \quad (43)$$

Figs. 13 and 14 (for the absolute value) display excellent agreement of Eq. (43) with simulations of CTRW

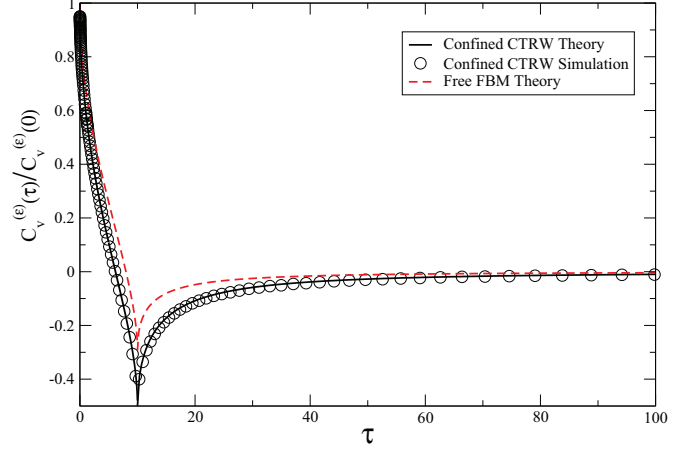


Figure 13: Normalised velocity autocorrelation function $C_v^{(\epsilon)}(\tau)$ for a free FBM process and a confined CTRW process with $\alpha = 0.5$. The CTRW simulations (\circ) were performed over the time range 10000 (a.u), and the system corresponds to a particle on a lattice with ten lattice points and reflecting boundaries. We chose $\epsilon = 10$ (a.u). The theoretical prediction for the CTRW ($—$) is given by Eq. (43), and for FBM ($-$) by Eq. (45).

subdiffusion for a lattice of size 10 with reflecting boundary conditions, and $\alpha = 1/2$. We observe that for confined motion the CTRW velocity autocorrelation function indeed attains negative values and has a minimum on $\tau = \epsilon$, as the confinement effectively induces correlations. For long τ the velocity autocorrelation function decays to zero (from the negative side) as the power-law

$$\frac{C_v^{(\epsilon)}(\tau)}{C_v^{(\epsilon)}(0)} \sim -\frac{1}{\Gamma(\alpha)\Gamma(1-\alpha)} \left(\frac{\epsilon}{\tau}\right)^{1+\alpha}, \quad (44)$$

valid for $\tau \gg \epsilon$.

B. Fractional Brownian Motion

For free FBM the position correlation function (10) together with the definition (40) produce the result

$$\frac{C_v^{(\epsilon)}(\tau)}{C_v^{(\epsilon)}(0)} = \frac{(\tau + \epsilon)^\alpha - 2\tau^\alpha + |\tau - \epsilon|^\alpha}{2\epsilon^\alpha}. \quad (45)$$

This function yields negative values for sufficiently long τ , and its minimum value $(2^{\alpha-1} - 1)$ is assumed at $\tau = \epsilon$. For long τ it decays toward zero from the negative side in the power-law form

$$\frac{C_v^{(\epsilon)}(\tau)}{C_v^{(\epsilon)}(0)} \sim -\frac{\alpha - \alpha^2}{2} \left(\frac{\epsilon}{\tau}\right)^{2-\alpha} \quad (46)$$

valid for $\tau \gg \epsilon$.

We see that both the velocity autocorrelation function of the confined CTRW and the one for free FBM acquire

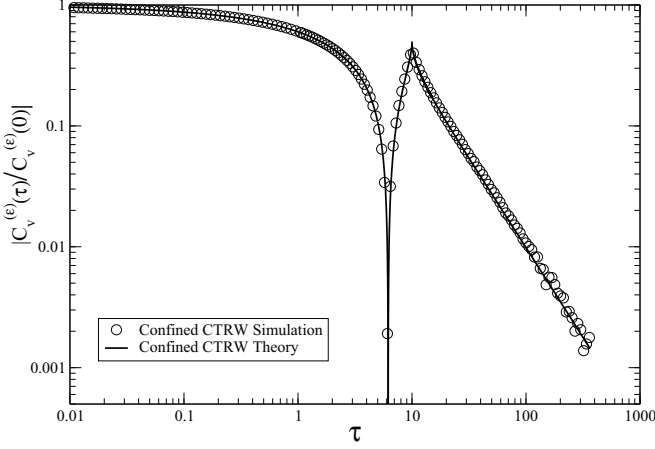


Figure 14: Absolute value of the normalised velocity autocorrelation function $C_v^{(e)}(\tau)$ for confined CTRW process with $\alpha = 0.5$. The CTRW simulations (\circ) are based on the parameters from Fig. 13. The theory line (—) corresponds to Eq. (43).

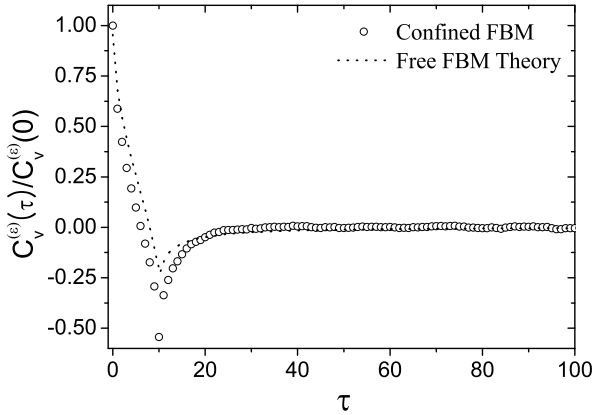


Figure 15: Normalised velocity autocorrelation function $C_v^{(e)}(\tau)$ for confined FBM with $\alpha = 0.5$. The simulations were performed on the interval $[-2, 2]$, and $\epsilon = 10$ (a.u.). For comparison, the velocity autocorrelation for free FBM is drawn based on Eq. (45).

negative values and decay as power-laws for large τ , see below. Further both obtain a sharp minimum for $\tau = \epsilon$. Confined FBM behaves similarly to free FBM, see Fig. 15. From our analysis it becomes clear that the shape of the velocity autocorrelation function may not be a good diagnosis tool to distinguish between subdiffusive CTRW and FBM processes. We note that for CTRW subdiffusion the time averaged correlation functions will be random variables, exactly like the time averaged mean squared displacement.

VII. DISCUSSION

The physical mechanisms leading to subdiffusion in biological cells or other complex systems are varied. The anomalous diffusion of inert biopolymers larger than some 10kD in living cells is due to molecular crowding, these are excluded volume effects in the viscoelastic, superdense cellular environment [30–32]. Potentially similar effects occur in single file diffusion: A tracer particle diffusing in a one dimensional channel and interacting with other Brownian particles will slow down its random motion, and subdiffusion with $\alpha = 1/2$ is observed [56]. What is the resulting motion like? Consider a particle, that gets repeatedly trapped during its random walk. Such trapping may give rise to a broad distribution of waiting times, as embodied in the CTRW model. Such broad distribution of trapping times could be due to chemical binding of the tracer particle to its environment on varied time scales, or due to active gelation/degelation of the crowding particles. Long-tailed trapping time distributions were observed for μm -sized particles due to interaction with a semiflexible actin mesh [22]. There, the anomalous diffusion exponent α depends on the size of the tracer particles versus the typical actin mesh size. Alternatively, motion patterns of FBM type may be due to coupling to the viscoelastic crowding environment [19]. Yet other approaches are based on polymer dynamics. De Gennes' reptation model of a polymer diffusing in a tube formed by foreign chains in a melt yields subdiffusion with $\alpha = 1/4$, and was used as a possible explanation of the short time dynamics of telomere motion [11].

One may speculate whether the widely observed subdiffusion of biomolecules and passive tracers is a mere coincidence of nature that should be attributed to the dense environment in the cell and/or to the wide distribution of obstacles and reactions in the cell. Or, maybe, subdiffusion is by itself a goal which was obtained via evolution? There exist claims that sub-diffusion is useful in certain cellular search strategies [9, 69]. One may also view subdiffusion to be a sufficiently slow process to help maintaining the organisation of the genome in the nucleus of the cell without the need for physical compartments [11]. Since reactions in many cases are controlled by diffusion, the emergence of slower-than-normal diffusion has far-reaching implications to signalling and regulatory processes in the cell. The standard theories of diffusion-controlled reactions under such circumstances must be replaced by subdiffusion-controlled reaction models. While these issues are clearly important, we here focused more on the characterisation of trajectories of single particles in the cell, in particular, as a quantitative diagnosis method to probe the nature of the stochastic motion in cells and other complex media.

Single particle tracking microscopy is a widely used technique. It allows one to locally probe complex systems in the liquid phase *in situ*. In particular it has become one of the standard tools in biophysical, colloidal, poly-

meric, and gel-like environments. The motion of tracers in these systems is often anomalous. Typically the experimentally recorded time series are evaluated in terms of the time averaged mean squared displacement $\overline{\delta^2(\Delta, T)}$. Here we collected the behaviour of $\overline{\delta^2(\Delta, T)}$ for the two most prominent anomalous stochastic processes, the continuous time random walk and fractional Brownian motion.

For CTRW subdiffusion, connected with ageing and weak ergodicity breaking, in an unconfined system the time averaged mean squared displacement scales linearly in time, $\overline{\delta^2(\Delta, T)}$ [Eq. (16)], renouncing the anomalous nature of the process. Only the dependence on the overall measurement time T pays tribute to the underlying subdiffusion. This behaviour contrasts the anomalous scaling $\langle x^2(t) \rangle = 2K_\alpha t^\alpha$ of the ensemble averaged mean squared displacement. Under confinement no plateau value is observed as in the ensemble average, instead, a power-law of the form $\overline{\delta^2(\Delta, T)} \simeq \Delta^{1-\alpha}$, Eq. (28), is found. Interestingly, this characteristic behaviour is approximately preserved when an appropriate cutoff in the waiting time is introduced. Conversely the distribution of the time averaged mean squared displacement around its ensemble mean becomes almost Gaussian in presence of the cutoff, while it has an exponential decay and a finite value at $\xi = 0$ when the system is non-ergodic and exhibits ageing.

FBM, in contrast, is ergodic, although ergodicity is reached algebraically slowly. Free FBM subdiffusion shows $\overline{\delta^2(\Delta, T)} \simeq \Delta^\alpha$, Eq. (18), while under confinement the plateau value of the ensemble average is reached, Eq. (30). For finite trajectories the distribution of the time averaged mean squared displacement is approximately Gaussian for short lag times.

Our analysis demonstrates how different the two stochastic processes are, despite sharing the same form of the ensemble averaged mean squared displacement. At the same time the velocity autocorrelation of confined CTRW subdiffusion is hardly distinguishable from that of FBM subdiffusion. Given a recorded time series

of anomalous diffusion from experiment it is important to know more precisely which stochastic process is responsible for the observed behaviour, in particular, with respect to diffusion-limited reactions, general transport behaviour, and related processes such as gene regulation. The analysis presented here, along with complementary tools discussed in Refs. [23, 59, 70], will be instrumental in the classification of anomalous diffusion behaviour.

Acknowledgments

We thank C. Selhuber-Unkel and L. Oddershede for providing the data used in Fig. 2, and for many useful discussions. Partial financial support from the Deutsche Forschungsgemeinschaft and the Israel Science Foundation is gratefully acknowledged.

Appendix A: Scatter distribution

Using the theory of Fox H -functions we obtain the exact form for the distribution $\phi_\alpha(\xi)$ of the dimensionless variable ξ [71]:

$$\phi_\alpha(\xi) = \frac{1}{\alpha^2 \xi} H_{1,1}^{1,0} \left[\frac{\xi^{1/\alpha}}{\Gamma(1+\alpha)^{1/\alpha}} \left| \begin{matrix} (0,1) \\ (0,1/\alpha) \end{matrix} \right. \right]. \quad (\text{A1})$$

This function has the series expansion

$$\phi_\alpha(\xi) = \frac{1}{\alpha \xi} \sum_{n=0}^{\infty} \frac{(-1)^n [\Gamma(1+\alpha)/\xi]^n}{n! \Gamma(-\alpha n)}, \quad (\text{A2})$$

and the asymptotic form

$$\phi_\alpha(\xi) \simeq \left(\xi^{1/\alpha} \right)^{(1-\alpha)/(2\alpha)-\alpha} \times \exp \left(-(1-\alpha) \left[\frac{\alpha^\alpha \xi}{\Gamma(1+\alpha)} \right]^{1/(1-\alpha)} \right) \quad (\text{A3})$$

valid at $\xi \gg \Gamma(1+\alpha)$.

-
- [1] C. Bräuchle, D. C. Lamb, and J. Michaelis, Editors, *Single Particle Tracking and Single Molecule Energy Transfer* (Wiley-VCH, Weinheim, 2010).
 - [2] M. J. Saxton and K. Jacobson, *Ann. Rev. Biophys. Biomol. Struct.* **26**, 373 (1997).
 - [3] M. J. Saxton, *Biophys. J.* **72**, 1744 (1997).
 - [4] H. Qian, M. P. Sheetz, and E. L. Elson, *Biophys. J.* **60**, 910 (1991).
 - [5] J. Perrin, *Comptes Rendus (Paris)* **146**, 967 (1908); *Ann. Chim. Phys.* **18**, 5 (1909).
 - [6] I. Nordlund, *Z. Physik. Chemie* **87**, 40 (1914).
 - [7] T. G. Mason and D. A. Weitz, *Phys. Rev. Lett.* **74**, 1250 (1995).
 - [8] W. J. Greenleaf, M. T. Woodside, and S. M. Block, *Ann. Rev. Biophys. Biomol. Struct.* **36**, 171 (2007).
 - [9] I. Golding and E. C. Cox, *Phys. Rev. Lett.* **99**, 098102 (2006).
 - [10] S. C. Weber, A. J. Spakowitz, and J. A. Theriot, *Phys. Rev. Lett.* **104**, 238102 (2010).
 - [11] I. Bronstein, Y. Israel, E. Kepten, S. Mai, Y. Shav-Tal, E. Barkai, and Y. Garini, *Phys. Rev. Lett.* **103**, 018102 (2009).
 - [12] G. Seisenberger, M. U. Ried, T. Endreß, H. Büning, M. Hallek, C. and Bräuchle, *Science* **294**, 1929 (2001).
 - [13] A. Caspi, R. Granek, and M. Elbaum, *Phys. Rev. Lett.* **85**, 5655 (2000).
 - [14] I. M. Tolić-Nørrelykke, E. L. Munteanu, G. Thon, L. Oddershede, and K. Berg-Sørensen, *Phys. Rev. Lett.* **93**, 078102 (2004).
 - [15] C. Selhuber-Unkel, P. Yde, K. Berg-Sørensen, and L. B. Oddershede, *Phys. Biol.* **6**, 025015 (2009).
 - [16] N. Gal and D. Weihs, *Phys. Rev. E* **81**, 020903(R) (2010).

- [17] D. Banks and C. Fradin, *Biophys. J.* **89**, 2960 (2005).
- [18] M. Weiss, M. Elsner, F. Kartberg, and T. Nilsson, *Biophys. J.* **87**, 3518 (2004).
- [19] J. Szymanski and M. Weiss, *Phys. Rev. Lett.* **103**, 038102 (2009).
- [20] J. Vercammen, G. Martens, and Y. Engelborghs, *Springer Ser. Fluoresc.* **4**, 323 (2007).
- [21] W. Pan, L. Filobelo, N. D. Q. Pham, O. Galkin, V. V. Uzunova, and P. G. Vekilov, *Phys. Rev. Lett.* **102**, 058101 (2009).
- [22] I. Y. Wong, M. L. Gardel, D. R. Reichman, E. R. Weeks, M. T. Valentine, A. R. Bausch, and D. A. Weitz, *Phys. Rev. Lett.* **92**, 178101 (2004).
- [23] J.-H. Jeon, V. Tejedor, S. Burov, E. Barkai, C. Selhuber, K. Berg-Sørensen, L. Oddershede, and R. Metzler (unpublished).
- [24] N. G. van Kampen, *Stochastic processes in physics and chemistry* (Elsevier, Amsterdam, 2007).
- [25] A. Y. Khinchin, *Mathematical foundations of statistical mechanics* (Dover Publications Inc., New York, NY, 2003).
- [26] Y. Sinai, *Theor. Prob. Appl.* **27**, 256 (1982); J. Dräger and J. Klafter, *Phys. Rev. Lett.* **84**, 5998 (2000).
- [27] V. Tejedor and R. Metzler, *J. Phys. A* **43**, 082002 (2010).
- [28] P. Siegle, I. Goychuk, and P. Hänggi, *Phys. Rev. Lett.* **105**, 100602 (2010).
- [29] R. Metzler and J. Klafter, *Phys. Rep.* **339**, 1 (2000); *J. Phys. A* **37**, R161 (2004); E. Barkai, *Phys. Rev. E* **63**, 046118 (2001).
- [30] S. B. Zimmerman and S. O. Trach, *J. Mol. Biol.* **222**, 599 (1991).
- [31] R. J. Ellis and A. P. Minton, *Nature* **425**, 27 (2003); A. P. Minton, *J. Cell Science* **199**, 2863 (2006).
- [32] S. R. McGuffee and A. H. Elcock, *PLoS Comput. Biol.* **6**, e1000694 (2010).
- [33] S. B. Yuste, G. Oshanin, K. Lindenberg, O. Bénichou, and J. Klafter, *Phys. Rev. E* **78**, 021105 (2008); E. Abad, S. B. Yuste, and K. Lindenberg, *Phys. Rev. E* **81**, 031115 (2010); I. M. Sokolov, S. B. Yuste, J. J. Ruiz-Lorenzo, and K. Lindenberg, *Phys. Rev. E* **79**, 051113 (2009); D. Froemberg and I. M. Sokolov, *Phys. Rev. Lett.* **100**, 108304 (2008).
- [34] Y. He, S. Burov, R. Metzler, and E. Barkai, *Phys. Rev. Lett.* **101**, 058101 (2008).
- [35] S. Burov, R. Metzler, and E. Barkai, *Proc. Natl. Acad. Sci. USA* **107**, 13228 (2010).
- [36] R. Metzler, V. Tejedor, J.-H. Jeon, Y. He, W. Deng, S. Burov, and E. Barkai, *Acta Phys. Polonica B* **40**, 1315 (2009).
- [37] S. Havlin and D. ben-Avraham, *Adv. Phys.* **36**, 695 (1987).
- [38] A. Klemm, R. Metzler, and R. Kimmich, *Phys. Rev. E* **65**, 021112 (2002); see also References therein.
- [39] E. W. Montroll and G. H. Weiss, *J. Math. Phys.* **10**, 753 (1969).
- [40] H. Scher and E. W. Montroll, *Phys. Rev. B* **12**, 2455 (1975).
- [41] H. Scher, G. Margolin, R. Metzler, J. Klafter, and B. Berkowitz, *Geophys. Res. Lett.* **29**, 1061 (2002); B. Berkowitz, A. Cortis, M. Dentz and H. Scher, *Reviews of Geophysics*, **44**, RG2003 (2006).
- [42] C. Monthus and J.-P. Bouchaud, *J. Phys. A* **29**, 3847 (1996); G. Ben Arous, A. Bovier, and V. Gaynard *Phys. Rev. Lett.* **88**, 087201 (2002).
- [43] E. Barkai and Y. C. Cheng, *J. Chem. Phys.* **118**, 6167 (2003).
- [44] J.-P. Bouchaud, *J. Phys. (Paris) I*, **2**, 1705 (1992); G. Bel and E. Barkai, *Phys. Rev. Lett.* **94**, 240602 (2005); A. Rebenshtok and E. Barkai, *ibid.* **99**, 210601 (2007); M. A. Lomholt, I. M. Zaid, and R. Metzler, *ibid.*, **98**, 200603 (2007); I. M. Zaid, M. A. Lomholt, and R. Metzler, *Biophys. J.* **97**, 710 (2009); F. D. Stefani, J. P. Hoogenboom, and E. Barkai, *Physics Today* **62**(2), 34 (2009); G. Margolin and E. Barkai, *Phys. Rev. Lett.* **94**, 080601 (2005); G. Aquino, P. Grigolini, and B. J. West, *EPL* **80**, 10002 (2007).
- [45] R. Metzler, E. Barkai, and J. Klafter, *Phys. Rev. Lett.* **82**, 3563 (1999); *Europhys. Lett.* **46**, 431 (1999). E. Barkai, R. Metzler, and J. Klafter, *Phys. Rev. E* **61**, 132 (2000); R. Metzler, J. Klafter, and I. M. Sokolov, *ibid.* **58**, 1621 (1998).
- [46] S. Burov and E. Barkai, *Phys. Rev. Lett.* **98**, 250601 (2007).
- [47] B. D. Hughes *Random Walks and Random Environments, Volume 1: Random Walks* (Oxford University Press, Oxford, 1995).
- [48] J.-P. Bouchaud and A. Georges, *Phys. Rep.* **195**, 127 (1990).
- [49] H. Scher, M. F. Shlesinger, and J. T. Bendler, *Phys. Today* **44**, No. 1, 26 (1991).
- [50] *Anomalous transport: foundations and applications*, edited by R. Klages, G. Radons, and I. M. Sokolov (Wiley-VCH, Weinheim, 2007).
- [51] A. N. Kolmogorov, *Dokl. Acad. Sci. USSR* **26**, 115 (1940); B. B. Mandelbrot and J. W. van Ness, *SIAM Rev.* **1**, 422 (1968); H. Qian, *Fractional Brownian Motion and Fractional Gaussian Noise*. In G. Rangarajan and M.Z. Ding (eds), *Processes with Long-Range Correlations* (Springer, Lecture Notes in Physics, Vol.621), pp.22-33.
- [52] R. Kubo, M. Toda, and N. Hashitsume, *Statistical Physics II: Nonequilibrium Statistical Mechanics* (Springer-Verlag, Heidelberg, 1995).
- [53] H. E. Hurst, *Trans. Am. Soc. Civ. Eng.* **116**, 400 (1951).
- [54] T. N. Palmer, G. J. Shutts, R. Hagedorn, F. J. Doblas-Reyes, T. Jung, and M. Leutbecher, *Annu. Rev. Earth Planet Sci.* **33**, 163 (2005).
- [55] I. Simonsen, *Physica A* **322**, 597 (2003); N. E. Frangos, S. D. Vrontos, and A. N. Yannacopoulos, *Appl. Stoch., Models Bus. Ind.* **23**, 403 (2007).
- [56] T. E. Harris, *J. Appl. Probab.* **2**, 323 (1965); L. Lizana and T. Ambjörnsson, *Phys. Rev. Lett.* **100**, 200601 (2008); L. Lizana, T. Ambjörnsson, A. Taloni, E. Barkai, and M. A. Lomholt, *Phys. Rev. E* **81**, 051118 (2010); E. Barkai and R. Silbey, *Phys. Rev. Lett.* **102**, 050602 (2009).
- [57] A. Taloni, A. V. Chechkin, and J. Klafter, *Phys. Rev. Lett.* **104**, 160602 (2010).
- [58] S.C. Kou and X. S. Xie, *Phys. Rev. Lett.* **93**, 180603 (2004); W. Min, G. Luo, B. J. Cherayil, S. C. Kou, and X. S. Xie, *Phys. Rev. Lett.* **94**, 198302 (2005).
- [59] M. Magdziarz, A. Weron, K. Burnecki, and J. Klafter, *Phys. Rev. Lett.* **103**, 180602 (2009). Compare also M. Magdziarz and J. Klafter, *Phys. Rev. E*, at press; K. Burnecki and A. Weron, *Phys. Rev. E* **82**, 021130 (2010).
- [60] A. Lubelski, I. M. Sokolov, and J. Klafter, *Phys. Rev. Lett.* **100**, 250602 (2008).
- [61] W. H. Deng and E. Barkai, *Phys. Rev. E* **79**, 011112

- (2009).
- [62] H. C. Fogedby, Phys. Rev. E **50**, 1657 (1994); A. Baule and R. Friedrich, Phys. Rev. E **71**, 026101 (2005); M. Magdziarz, A. Weron, and J. Klafter, Phys. Rev. Lett. **101**, 210601 (2008); M. Magdziarz, A. Weron, and K. Weron, Phys. Rev. E **75**, 016708 (2007); E. Heinsalu, M. Patriarca, I. Goychuk, G. Schmid, and P. Hänggi, Phys. Rev. E **73**, 046133 (2006).
 - [63] T. Neusius, I. M. Sokolov, and J. C. Smith, Phys. Rev. E **80**, 011109 (2009).
 - [64] J.-H. Jeon and R. Metzler, Phys. Rev. E **81**, 021103 (2009).
 - [65] O. Y. Sliusarenko, V. Y. Gonchar, A. V. Chechkin, I. M. Sokolov, and R. Metzler, Phys. Rev. E **81**, 041119 (2010).
 - [66] I. M. Sokolov, E. Heinsalu, P. Hänggi, and I. Goychuk, EPL **86**, 30009 (2009).
 - [67] J.-H. Jeon and R. Metzler, J. Phys. A **43**, 252001 (2010).
 - [68] A. Baule and R. Friedrich Eur. Phys. Lett. **77**, 10002 (2007).
 - [69] G. Guigas and M. Weiss, Biophys. J. **94**, 90 (2008).
 - [70] V. Tejedor, O. Bénichou, R. Voituriez, R. Jungmann, F. Simmel, C. Selhuber, L. Oddershede, and R. Metzler, Biophys. J. **98**, 1364 (2010).
 - [71] A. M. Mathai and R. K. Saxena, The H-function with Applications in Statistics and Other Disciplines (Wiley Eastern Ltd., New Delhi, 1978); A. M. Mathai, R. K. Saxena, and H. J. Haubold, The H-function, Theory and Applications (Springer, New York, 2010).